IOSR Journal of Applied Geology and Geophysics (IOSR-JAGG)
e-ISSN: 2321–0990, p-ISSN: 2321–0982.Volume 3, Issue 4 Ver. II (Jul - Aug. 2015), PP 49-64
www.iosrjournals.org

Integrated Geophysical Studies Over Parts of Central Cross River State for the Determination of Groundwater Potential and Foundation Properties of Rocks

V. I. Obianwu[1,] , A. O. Egor[2,] , A. A. Okiwelu[3] and E. D. Ebong[4]
[1,3,4]Department of Physics (Geophysics Unit), University of Calabar, P.M.B. 1115, Calabar, Nigeria
[2]Department of Physics, Cross River University of Technology, Calabar, Nigeria

Abstract: *A total of 71 Vertical Electrical Soundings were carried out using Schlumberger electrode configuration for the evaluation of groundwater potential in parts of central Cross River State, Nigeria. Interpretation of data showed three to six geoelectric layers. Productive shallow and deep aquifer zones were identified at depths of 60 m and 150 m respectively, corresponding to a resistivity range of 100-500 Ωm for shallow aquifers and 1000-2500 Ωm for deep aquifers respectively. The lithologic data of the aquifers revealed sand/sandstone and very coarsed grained sand/fractured basement, respectively. Seismic refraction survey was also carried out within the same study area for the foundation study of rocks. The studies revealed an average thickness of 4.5 m (probably sand/clay) and 10.0 m (probably gravelly sand/shale) for the first and second layers respectively. The range of velocities for the first three layers are 602 m/s to 960 m/s, 378 m/s to 2,424 m/s and 1,587 m/s to 5,368 m/s, respectively, indicating that the soils in the area are not homogeneous. It is inferred from the relative high values of calculated elastic constants in most of the locations, that the soils are well consolidated and as such suitable for large engineering construction in such locations, while in the rest of the locations the soils are considered unconsolidated and unsuitable for large construction work due to the relative low values of the elastic constants.*

Keywords: *Vertical Electrical Sounding, groundwater, electrical resistivity, aquifer, electrode separation, refractor, geoseismic section.*

I. Introduction

The central parts of Cross River State forms a part of the geopolitical and geographic entity where the Cross River State Government dissipated so much energy to upgrade its natural and human resources. Since the commencement of the democratic experiment in 1999, the Cross River State Government initiated the Urban Renewal Scheme, which led to the improvement of facilities in some urban centres in the state. A corresponding population growth within those urban centres, which include Yakurr and Ikom Local Government Areas form a part of the study area. In another policy of the state government tagged: "Rural Development Policy", the emphasis on development was shifted to the rural communities which constituted the bulk of the state population. These two policies resulted in population increase within the urban centres and the rural areas which has put so much pressure on the available water supply. The situation is further worsened by the overstretching of the available facilities and hence the development and expansion of water facilities to meet present and future demands of the communities in the study area have become very expedient. Although for over a decade, there had been some effort to develop and expand these facilities, especially in the area of exploitation of ground water, most of these boreholes have since stopped producing as revealed by presence of failed boreholes and manually dug wells in some of the Local Government Areas in the study area.

The consequence of failed wells is that greater parts of the population depend on surface water sources like rivers and streams which are both seasonal and prone to contamination leading to water borne diseases like guinea worm, bilhaziosis, typhoid, and cholera during the dry season. In the light of the above, it is essential to acquire a geophysical and hydrogeological database that will help in site and groundwater development in the study area leading to the present study.

Electrical resistivity method and seismic refraction method are efficient tools for site investigation towards the determination of overburden thickness, bed rock competence and mapping of subsurface structures before excavation and construction (Kurthenecker, 1934; Drake, 1962; Early and Dyer, 1964; Burton 1976; Nun, 1979; Keary and Brooks, 1984; Olorunfemi and Meshida, 1987). Both methods can be used in geotechnics to assess the rock strength, determine rippability and potential fluid content (Ayolabi, 2004; Ayolabi *et al.*, 2008). In the present study, the electrical resistivity method and seismic refraction methods were deployed to determine the ground water potentials and foundation condition of rocks within the study area.

II. Geology And Hydrogeology Of The Study Area

The study area covering the central part of Cross River State lies between latitudes 5°45′ N and 6°28′ N and longitudes 8°00′ E and 9°11′ E. The area includes the Ikom-Mamfe embayment and Boki Geological environment. The Ikom-Mamfe embayment is the Northwest to Southeast segment of the Northeast to Southwest trending Benue Trough. It extends laterally into parts of Western Cameroon, where it covers an area of 2,016km^2 (Eseme *et al*., 2002). It occupies the low lying areas between the Oban Massif and the Obudu plateau in Cross River State, Nigeria and is characterized by low relief and gently undulating topography (Eseme *et al*., 2002) (see Fig. 1). This basin covers some of the communities in Abi, Yakurr, Obubra, Ikom and Etung Local Government Areas, which constitute part of the study area.

The Precambrian basement rocks under the Ikom-Mamfe basin -are overlain by three major cretaceous lithostratigraphic units comprising the Asu River Group (ARG), Eze Aku Group (EAG) and the Post-Semtonian Nkporo-Afikpo shale formation (NASF) (see Fig. 1). Some isolated alluvial deposits are also found along parts of Cross River plains, while tertiary volcanic rocks like basalts and dolerites intrude into the overlying cretaceous sedimentary units in some locations (Benkelil *et al*., 1975; Offodile, 1975; Cross River State Basin Development Authority (CRBDA), 1982; NGSA, 2006) (see Fig. 1).

Migmatitic granitic gneisses, schists and pegmatite are the crystalline basement rocks in the basin. The gneisses are usually foliated with some pink feldspars and vary from fine homeblende, black to white with porhyroblastic feldspars. The albian ARG is the oldest sedimentary rocks in the study area and directly overlie the Precambrian basement; they are basically non-marine to marginal marine in character and predominantly cover the eastern part of the study area. The sediments within the ARG consist of impervious shales, limestone with some sandstone intercalation and ammonites (Nigerian Geological Survey Agency (NGSA), 2006; Odigi and Amajor, 2009). The EAG comprises of thick flaggy impervious calcareous and non-calcareous shales, sandy shally limestone and calcareous sandstone (NGSA, 2006; Odigi and Amajor, 2009). The EAG is overlain by the post santonian NASF which occupy most of the western parts of the study area. Sandstone, mudstone and shale are the major lithologic units in the formation (NGSA, 2006; Odigi and Amajor, 2009). The shales are often carbonaceous and pyritic which is suggestive of sediments that were deposited in a poorly oxygenated shallow water environment with restricted air circulation (Peters *et al*., 1987).

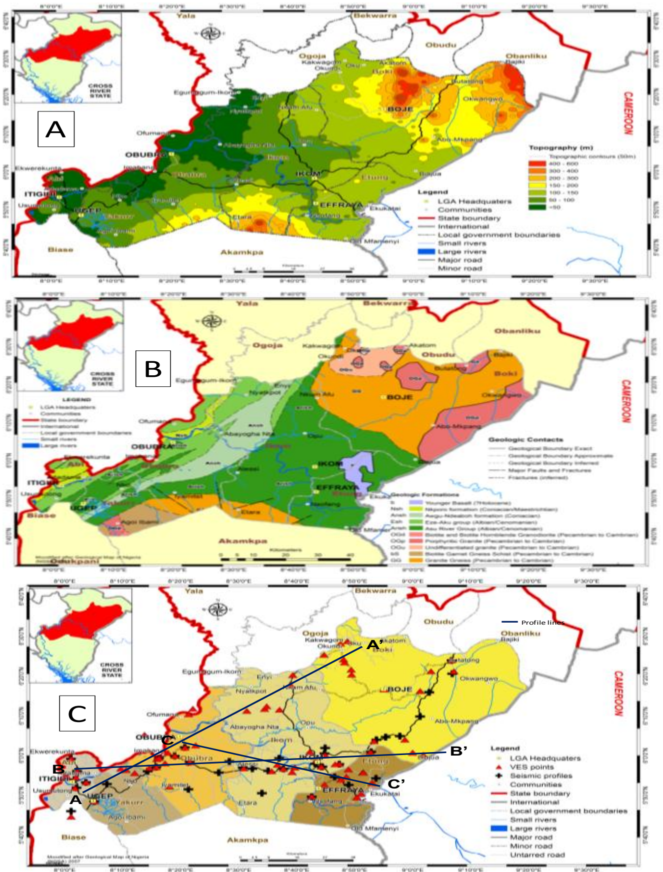

Fig. 1: (A) Topographic map of Central Cross River State showing the elevation, (B) Geological map of the study area and (C) Location map of the study area showing the seismic stations and VES points (Redrawn from NGSA, 2006)

The Cross River Basin Development Authority (CRBDA), carried out a geological segmentation in 1982 and on this basis, Peters (1989) identified four shallow hydrogeological provinces consisting of the crystalline basement province (CBP), Cross River Plain Province (CRPP), Nkporo-Afikpo Shales Province (NASP) and Alluvial/Buried River Province (ABRP). The area exhibits a dendritic drainage pattern which is drained by the Cross River and some of its tributaries including Ovarr, Okwo, Lokpoi, Okang, Udip, Ujidam, Okpon, Atimaka, Aboine, Otere, Usee and Nde River (See Fig. 1B).

The study area's vegetation is that of the guinea savannah, this is characterized by a mixture of green plants, shrubs, grasses and trees, it has two seasons – wet (March to October) and dry (November to April). Annual precipitation is usually over 2,200m while annual temperature ranges between 32 °C to 36 °C. Average relative humidity is about 85 per cent. Recently, significant shift in both the upper and lower boundaries of these two climatic conditions have been observed (Martinez *et al*., 2008; Rapti-Caputo, 2010; Riddell *et al*., 2008; Wagner and Zeck-hauser, 2011).

Basalts, dolerites and major rock types in the CBP are distributed in patches in many parts of the study area, although the southern part of the study area is dominated by gneissic materials which is another major rock type in the CBP region. The occurrence of groundwater in the CBP is facilitated by the presence of secondary structures like fracture, faults, joints, fissures and other weathered litho-units. Ground water from these structures can occur even at depths as low as 50m with poor in yield at some locations (Edet *et al*., 2011; Offiong, 2011; Akpan *et al*., 2013). The single largest hydrogeological province is the CRPP covering the northern, central, southwestern and Northwestern parts of the study area. The aquiferous units in this province consist of deformed shales, siltstones, limestones and sandstones of Markurdi formation (Petters, 1989).

The NASP occupied the western part of the study area and consists basically of porous sandstones, compact shales, mudstones, marls and clays (Petters, 1989; Nigerian Geological Survey Agency (NGSA), 2006). The permeable sandstone appears to be an eastward extension of the adjoining Afikpo sandstones (Petters, 1989; Odoh, 2010). Most of the litho-units are porous and thus act as high yielding aquifers (Akpan *et al.*, 2013).

III. Methods Of Data Collection

Resistivity method

Conventional Schlumberger array VES (Telford *et al*., 1990) with the maximum electrode spacing (AB) of 800 m at some of the 71 sites. The depth of current penetration using Schlumberger electrode array is ⅓ to ¼ of AB/2 which comes to 133m to 150m is deemed sufficient to know about the aquifer and bedrock properties (Bernard, 2003; Roy and Apparao, 1971). The soundings were constrained by data from existing boreholes located near some of the VES points.

Seismic method

Ten profile lines were laid in each of the local government areas in the central part of the state. Each profile line was 60 m long with inter-geophone spacing of 5m (see Fig. 9). Inter-profile line spacing varied from 1.5 km to 3 km. The P- waves and S-waves were mechanically generated using the sledge-hammer perpendicular to a base plate that is placed on a flat surface.

The arrival time of signals in each of the geophones are picked from the record of the seismograph. Other details of the refraction survey procedures have been documented by Ayolabi (2004).

IV. Results

Resistivity survey

The initial analysis of the VES data began with the computation of apparent resistivities, using the Schlumberger array equation as expressed below:

$$\rho_{as} = \frac{\left(\frac{AB}{2}\right)^2 - \left(\frac{MN}{2}\right)^2}{MN}\frac{\Delta V}{I} \quad = \frac{\pi b^2 R}{4a} \qquad (1)$$

where ρ_{as} is the Schlumberger apparent resistivity, AB is the current electrode distance, MN is the potential electrode distance, R is the apparent resistance ΔV is the voltage and I is current. The calculated ρ_{as} of each sounding station was plotted against half of the current electrode spacing $AB/2$ on a log-log graph paper, VES curves were obtained and noisy segments were removed by manual smoothening (Bhattacharya, 1968; Chakravarthi *et al*., 2007). The smoothened curves were quantitatively interpreted in terms of true resistivity and thickness by a conventional manual curve matching procedure using master curves and auxiliary charts (Orellana and Moony, 1966).

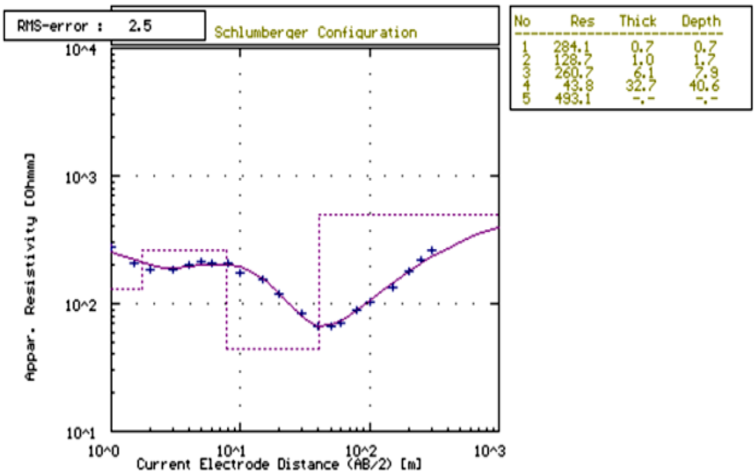

Fig. 2: Apparent Resistivity model curve of Abankang in the study area

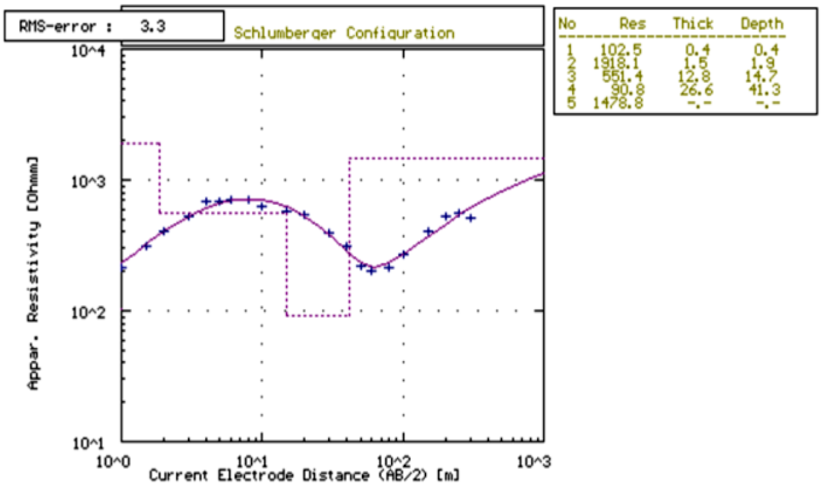

Fig. 3: Apparent Resistivity model curve of Abia Bendeghe in the study area

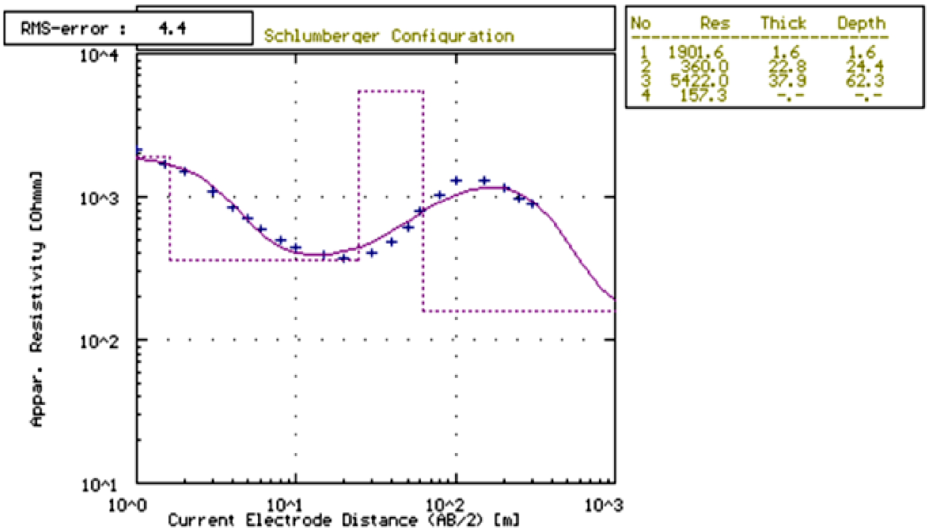

Fig. 4: Apparent Resistivity model curve of Abu Ogbagante in the study area

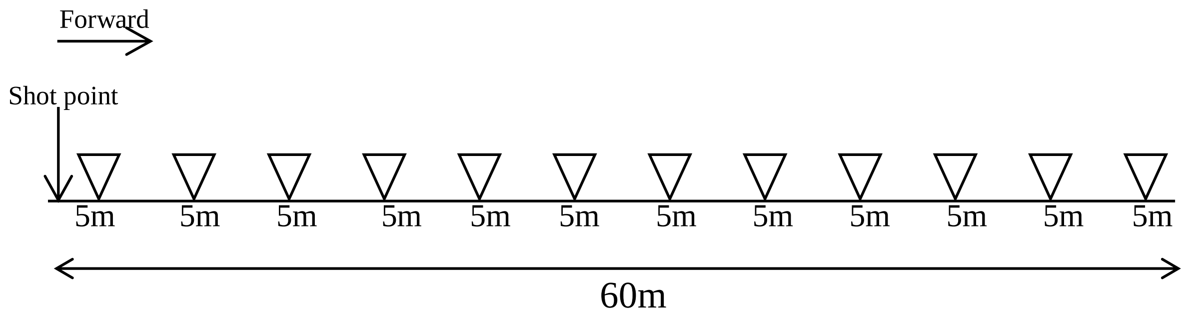

Fig.5: Geophone layout for seismic refraction data acquisition

Computer software Resist was used to refine the manually interpreted results (Vender Velpen, 1988; Zohdy, 1989; Loke, 2001). The layer parameters (apparent resistivity, layer thickness and depth) realized initially from the manual interpretation stage were used as inputs into the computer modeling software. The modeled data was iterated to obtain high accuracy by consciously ensuring that the root mean square error does not exceed 5%. The results are displayed in Table 1 (a, b & c).The field curves revealed 3 to 5 interpretable geo-electric layers resembling KH, HKH, HK, K, KHKH, KQ, KQH, KHH, AKQ, KAKH, Q, QQ, QQQ, AAK, AAKH, QH, HKQ, KQQ, QQH, and KKH types, as shown in Figs. 3-5. VES stations 6, 12, 26, 29, 36, 37, 45, 46, 47 and 60 have revealed reflection coefficients more than 0.9 and resistivity contrasts more than 0.9 and 19, respectively.

Seismic survey

The first arrival time from each geophone (5m apart) was plotted between the geophone numbers versus the arrival time of P-waves and S-waves for each shooting point for forward and reverse arrivals (Fig. 5) (Geosoft, 2001). The first arrival time was picked from these plots (seismic wiggles) (see Figs. 6 & 7). A time-distance plot was generated for P-wave and S-wave using a software SeisImager. The layer velocities and depths for P-waves and S-waves are displayed automatically with the T-X plots (see Fig. 8 – 10).

Although the software simplifies the process of analysing the data by its automation procedure the underlying principle for calculating the velocity and depth of the layers was based on the Wyrobek Method (Telford et al., 1990). The Wyrobek's method upon which the SeisImager software is based does not actually require reverse profiles because the intercept at a shotpoint does not depend on the direction in which the cable is laid (Telford et al., 1990). The summary of the seismic refraction velocity results is given in Table 2 (a & b), while the computed results of the elastic constants are in Tables 3 (a & b).

V. Discussion

Geoelectric Sections

A first glance, the apparent resistivity curves (see Fig. 2 – 4), reveal 3 - 6 layers that are characterized by low to moderately high resistivity values. The first layer which is exposed at the surface is characterized by electrical resistivity values that are generally less than 500 Ωm (that is ρ_1 < 500 Ωm) except at a few VES points (VES 5, VES 28, VES 33, VES 34, VES 41, VES 50, VES 52, VES 54, VES 55, VES 56, VES 60, VES 62 VES 66, and VES 70) where the electrical resistvity values are moderately high with ρ_1 >500 Ωm as a result of the presence of gravel on the surface .The thickness of the first layer lie between 0.4m to 5.8m. At some locations where thickness of 5m was observed, the rock bears water and the yield can sustain hand dug wells, especially during the rainy season.

The second geoelectrical layer is dominated by clay/shale with thickness of 2.6 – 10.2 m and resistivity of 90 – 1,547 Ωm. However at VES 21 and VES 22, the least values of resistivity was recorded between 9.4-12.6 Ωm, this particular section of the layer was delineated as shale. The shales are thick in some locations and the observed shale content of this layer suggests that primary porosity will be very low and consequently, water transmission and storage will be very poor (Odoh, 2010).

The electrical resistivity values of the third layer varied between 164 – 746 Ωm, with thickness of 5.8 – 38 m corresponding to the variability of the lithology. Layers with resistivity values less than 30 Ωm are inferred to be responses from wet clays while electrical resistivity values of over 500 Ωm are attributed to sandy/sandstone materials which correlate well with lithology of nearby boreholes where sandy materials dominate the subsurface composition in this layer. The sands are usually saturated with water and forms the aquifer (Edet et al., 2011; Akpan et al., 2013).

Some locations like Ofunbongha and Adun Beach did not reveal fourth layer whereas in locations like Ntamante, the electrical resistivity values is quite high (ρ_4 > 8000 Ωm) which is indicative of basement rocks. The fifth layer was touched at Abakang , Alok and Nsadop, the electrical resistivity values ranges from 459.9 – 1340 Ωm and thickness between 40 m and 110 m.

TABLE 1(a) Summary of results of geo-electric parameters for VES 5-19

Location / VES Station number	Number of layer	Geo-electric layer Resistivities (Ohm-m)						Geo-electric Layer Thicknesses (m)						Depth to bottom of Geoelectric layers (m)				
		ρ_1	ρ_2	ρ_3	ρ_4	ρ_5	ρ_6	d_1	d_2	d_3	d_4	d_5	d_6	h_1	h_2	h_3	h_4	h_5
Itigidi /1	**5**	120.0	250.0	169.0	80.0	300.0	-	2.1	3.6	26.1	31.5	-	-	2.1	5.7	31.8	63.3	-
Ediba /2	**4**	70.0	186.0	280.0	49.0	-	-	0.9	7.2	26.9	-	-	-	0.9	8.1	34.0	-	-
Ekureku /3	**5**	50.0	110.0	206.0	118.0	50.0	-	1.1	2.6	5.2	10.2	-	-	1.2	3.7	8.8	19.0	-
Agbara /4	**5**	306.0	350.0	180.0	40.0	16.0	-	0.6	1.2	6.7	5.1	-	-	0.6	1.8	8.9	14.0	-
Ugep-Ijiman / 5	5	1628.2	313.2	748.8	71.4	546.9	–	0.5	1.6	2.5	32.4	-	–	0.5	2.1	4.6	36.9	
Iyamoyong/Iyametet Rd /6	5	216.8	143.5	116.8	129.0	11.2	–	1.0	1.5	5.0	18.0	–	–	1.5	2.5	7.5	25.5	–
Egbezium / 7	5	15.8	156.6	1396.9	1052.0	501.0	–	1.7	3.8	17.5	26.6	–	–	1.7	5.5	22.9	48.6	–
St. Thomas P/S Ugep / 8	5	400.0	701.2	250.1	27.0	80	–	1.0	1.5	6.0	42.0	–	–	1.0	2.5	8.5	50.5	–
Lokpoi / 9	5	144.9	25.3	141.0	23.3	302.5	–	0.6	3.2	11.9	38.8	–	–	0.6	3.7	15.6	54.4	–
Assigha / 10	5	172.4	30.9	167.1	10.6	2477.0	–	1.4	13.5	13.1	27.0	–	–	1.4	14.9	28.1	65.1	–
Nyima / 11	4	142.2	38.3	101.0	26.8		–	0.9	4.1	36.9		–	–	0.9	5.1	42.0		–
Onyadama /12	5	340.2	360.7	160	20.12	80.11	–	1.0	1.50	5.0	20	–	–	1.0	2.5	3.6	6.7	–
Ababene / 13	6	49.0	52.3	150	24.6	38.4	37.2	1.0	1.5	1.1	3.1	34.9	–	1.0	2.5	3.6	6.7	41.6
Ijutum-Eja Road / 14	3	62.9	144.2	124.4	–	–	–	4.2	33.5	–	–	–	–	4.2	37.7	–	–	–
Adun Beach / 15	3	51.2	90.0	15.4	–	–	–	0.5	33	–	–	–	–	0.5	33.5	–	–	–

TABLE 1(b) Summary of results of geo-electric parameters for VES 20-34

Location / VES Station number	Number of layer	Geo-electric layer Resistivities (Ohm-m)						Geo-electric Layer Thicknesses (m)						Depth to bottom of Geoelectric layers (m)				
		ρ_1	ρ_2	ρ_3	ρ_4	ρ_5	ρ_6	d_1	d_2	d_3	d_4	d_5	d_6	h_1	h_2	h_3	h_4	h_5
Okorokpana / 16	6	60.0	25.0	35.0	70.0	25.0	150.0	1.0	1.5	3.0	13.0	50.0	–	1.0	2.5	5.5	18.5	68.5
Apiapum / 17	6	60.3	533.5	164.5	3197.7	121.4	1770.2	1.0	2.0	7.0	20.0	40.0	–	1.0	3.0	10.0	30.0	70.0
Imabana / 18	5	561.2	384.2	73.2	21.4	-	–	0.8	9.2	13.8	17.2	–	–	0.8	10.0	23.8	41.0	–
Owakande 2 / 19	4	200.0	500.0	1200.0	500.0	–	–	1.2	15.0	75.0	–	–	–	1.2	16.2	91.2	–	–
Ofunbongha / 20	3	35.1	263.4	97.5	28.4	–	–	5.9	27.1	39.8	–	–	–	5.9	33.0	72.8	–	–
Ogurude / 21	5	50.0	16.0	292.1	74.3	147.5	–	1.0	5.6	35.3	76.8	–	–	1.0	6.5	41.8	118.6	–
Ogurude-Eda Rd / 22	3	153.8	9.4	180.4	–	–	–	1.7	54.6	–	–	–	–	1.7	56.3	–	–	–
Ohanne-Eda / 23	5	168.7	12.6	17.5	7.2	23.9	–	0.9	7.5	18.7	28.7	28.4	–	0.9	8.5	27.2	55.6	–
Ofio-Oji / 24	5	268.4	237.8	188.3	77.0	39.7	–	0.9	4.9	17.6	82.4	–	–	0.9	5.8	23.4	105.7	–
Okimbongha / 25	3	10.5	149.5	19.7	–	–	–	4.3	59.6	–	–	–	–	4.3	63.9	–	–	–
Iyamoyong / 26	5	96.0	1063.0	116.8	129.0	11.2	–	0.7	5.0	33.8	49.6	–	–	0.7	5.7	39.5	89.2	–
Edondon / 27	4	34.0	14.2	132.0	33.2	–	–	1.4	5.1	24.6	–	–	–	1.4	6.5	31.1	–	–
Iyamitet / 28	5	558.6	115.5	21.0	250.0	24.5	–	0.8	3.20	14.5	34.2	–	–	0.8	4.0	18.5	52.6	–
Onyenokpon / 29	6	160.1	806.2	28.0	56.7	8.4	62.4	0.7	2.3	14.9	24.1	61.0	–	0.7	3.1	18.0	42.1	103.1
Usumutong / 30	4	447.0	859.0	746.0	60.0	-	-	5.1	10.8	36.0	-	–	-	5.1	15.9	51.9		–

TABLE 1(c) Summary of results of geo-electric parameters for VES 35-49

Location / VES Station number	Number of layer	Geo-electric layer Resistivities (Ohm-m)						Geo-electric Layer Thicknesses (m)						Depth to bottom of Geo-electric layers (m)				
		ρ_1	ρ_2	ρ_3	ρ_4	ρ_5	ρ_6	d_1	d_2	d_3	d_4	d_5	d_6	h_1	h_2	h_3	h_4	h_5
Ekporkpa / 31	4	390.0	206.0	57.3	1866.5	–	–	2.9	2.5	72.5	–	–	–	2.9	5.4	78.3	–	–
Okuni / 32	4	288.7	1235.8	195.4	338.2	–	–	1.0	6.9	28.0	–	–	–	1.0	7.9	36.0	–	–
Okuni-Okoroba Rd / 33	4	1354.0	2761.0	255.0	6415.0	–	–	0.9	3.0	68.8	–	–	–	0.9	3.9	72.8	–	–
Abijang / 34	4	1319.7	2606.5	225.1	6030.3	–	–	0.8	3.3	68.8	–	–	–	0.8	4.1	73.8	–	–
Okuni-Ikom Road / 35	4	396.7	70.6	500.0	30.0	257.0	–	1.5	6.6	4.8	65.5	–	–	1.5	8.1	12.8	78.4	–
Grass Field / 36	4	84.8	592.8	181.6	62.1	–	–	0.9	8.5	27.3	–	–	–	0.9	9.5	36.7		–
Keteme-Boarder Road / 37	4	126.4	1054.6	83.4	1638.7	–	–	0.4	4.1	77.6	–	–	–	0.4	4.5	82.1	–	–
Mbetim Efraya / 38	5	72.4	223.2	15.8	755.1	48.3	–	0.6	0.5	2.4	10.5	–	–	0.6	1.1	3.5	14.0	–
Last Motor / 39	5	310.0	90.0	825.0	237.0	56.0	–	0.6	0.8	12.4	39.7	–	–	0.6	1.4	13.8	53.5	–
Ajassor / 40	5	326.2	81.9	512.0	240.0	50.0	–	1.0	4.3	8.5	42.0		–	1.0	5.3	13.8	55.8	–
Ajassor Junction / 41	4	712.0	75.6	308.3	84.6	–	–	1.8	2.3	14.2	–	–	–	1.8	4.1	18.3	–	–
Ejago-Kura / 42	4	163.8	40.9	323.4	54.3	–	–	4.6	53.7	18.2	–	–	–	4.6	58.2	77.4	–	–
Etomi / 43	5	78.3	1816.0	1653.0	52.1	173.8	–	0.4	0.7	3.7	221.2	–	–	0.4	1.1	4.8	226.0	–
Abia-Bendeghe Road / 44	5	102.0	1919.1	551.4	90.8	1478.0	–	0.4	1.5	12.8	26.6	–	–	0.4	1.9	14.7	41.3	–
Ekigatia / 45	5	52.0	967.5	136.8	15.0	119.3	–	0.5	7.7	22.3	38.2	–	–	0.5	8.2	30.6	68.7	–

TABLE 1 (d) Summary of results of geo-electric parameters for VES 50-64

Location / VES Station number	Number of layer	Geo-electric layer Resistivities (Ohm-m)						Geo-electric Layer Thicknesses (m)						Depth to bottom of Geoelectric layers (m)				
		ρ_1	ρ_2	ρ_3	ρ_4	ρ_5	ρ_6	d_1	d_2	d_3	d_4	d_5	d_6	h_1	h_2	h_3	h_4	h_5
Agbokim Water Fall / 46	4	45.7	725.5	37.5	90.1	–	–	0.9	13.4	46.9	–	–	–	0.9	14.3	61.2	–	–
Adijikpong / 47	4	163.8	40.9	3234.0	54.3	–	–	4.6	53.6	18.2	–	–	–	4.6	58.2	71.4	–	–
Bendeghe Ekim / 48	3	1526.8	121.4	1571.0	-	–	–	3.1	37.9	-	–	–	–	3.1	40.0	-	–	–
Otere Ikom / 49	4	18.2	188.6	61.2	254.1	–	–	0.4	5.1	31.2	–	–	–	0.4	5.5	36.6	–	–
Orimekpang / 50	5	1085.3	119.1	1465.8	63.5	18058.0	–	0.5	0.7	2.5	12.6	–	–	0.5	1.2	3.7	16.3	–
Biajua / 51	4	360.5	298.7	264.0	5624.3	–	–	0.5	2.0	110.0	–	–	–	0.5	2.5	112.5	–	–
Bashua / 52	5	985.0	162.8	2091.7	57.1	35111.2	–	0.6	1.3	3.2	16.2	–	–	0.6	1.9	5.1	21.4	–
Danare / 53	4	287.1	2368.4	240.0	3082.0	–	–	0.5	9.5	144.7	–	–	–	0.5	10.0	154.6	–	–
Abu Ogbangante / 54	4	1801.6	360.0	5422.0	157.3	–	–	1.6	22.8	37.9	–	–	–	7.6	24.4	62.3	–	–
Kanyang / 55	5	1084.0	4317.3	348.6	953.8	1701.0	–	0.4	0.8	8.9	23.1		–	0.4	1.2	10.1	33.2	–
Wula / 56	6	1581.6	2213.9	314.3	13655.0	1240.0	6103.4	0.6	3.7	6.1	28.6	8.7	–	0.6	4.2	10.3	38.9	126.6
Nkum Yala/ 57	6	163.5	454.1	51.2	148.8	21.4	41.8	0.7	12.0	9.9	32.8	31.0	–	0.7	12.7	22.6	55.4	86.4
Mile 3 – Nsele / 58	4	129.8	24.5	58.0	17.4	–	–	0.7	15.8	100.8	–	–	–	0.7	16.4	117.2	–	–
Govisco / 59	4	390.0	206.0	57.0	1866.0	–	–	2.9	2.5	72.0	–	–	–	2.9	5.4	77.4	–	–
Edor / 60	6	1685.0	166.1	259.0	179.3	36.0	663.4	1.4	3.8	36.4	22.0	54.3	–	1.4	5.2	41.6	63.6	117.9

TABLE 1 (e) Summary of results of geo-electric parameters for VES 61-71

Location / VES Station number	Number of layer	Geo-electric layer Resistivities (Ohm-m)						Geo-electric Layer Thicknesses (m)						Depth to bottom of Geoelectric layers (m)				
		ρ_1	ρ_2	ρ_3	ρ_4	ρ_5	ρ_6	d_1	d_2	d_3	d_4	d_5	d_6	h_1	h_2	h_3	h_4	h_5
Abankang / 61	5	284.1	128.2	260.7	43.8	493.1	–	0.7	1.0	6.1	32.7	–	–	0.7	1.7	7.8	40.6	–
Alok / 62	5	601.5	1547.0	415.0	60.8	459.9	–	0.5	3.1	20.1	117.1	–	–	0.5	3.6	23.7	140.8	–
Ntamantet / 63	4	71.4	671.6	119.6	8341.0	–	–	0.4	1.0	23.9	–	–	–	0.4	1.4	25.3	–	–
Bafin Etimtim / 64	4	186.7	249.7	144.0	1180.0	–	–	1.1	12.9	41.8	–	–	–	1.1	12.9	41.8	–	–
Ogep Osokom / 65	4	188.3	415.2	220.4	3798.4	–	–	1.8	8.4	39.0	–	–	–	1.8	10.2	48.2	–	–
Bansan Osokom / 66	5	2115.0	600.3	3282.0	373.8	3549.3	–	1.0	1.7	3.4	13.6	–	–	1.0	2.7	6.1	18.8	–
Obubra Bansan / 67	5	448.2	748.1	218.0	2719.0	1016.8	–	0.7	2.9	12.3	65.6	–	–	0.7	3.6	15.8	81.6	–
Nsadop / 68	6	53.4	345.6	229.7	1358.0	1340	6430.0	4.6	53	18.2	21.9	24.2	–	4.6	58	75.8	97.7	121.9
Kakwagom / 69	5	486.4	104.0	575.1	121.8	993.3	–	0.7	2.6	4.7	35.3	–	–	0.7	3.3	8.0	43.3	–
Boje / 70	5	672.0	461.2	758.6	413.1	3506.0	–	0.8	2.6	5.5	18.4	–	–	0.8	3.4	8.8	28.3	–
Edondon / 71	5	218.0	254.0	291.0	65.0	38.0	–	1.2	5.3	24.0	53.0	–	–	1.2	6.5	30.5	83.5	–

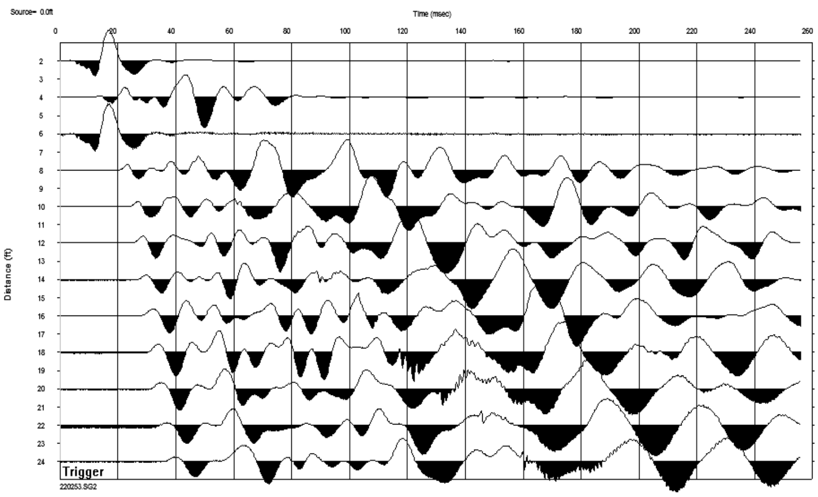

Fig. 6: Seismic wiggle showing forward arrival time of P-wave curve for a 12-channel seismic line installed to the Seismic equipment from the study area

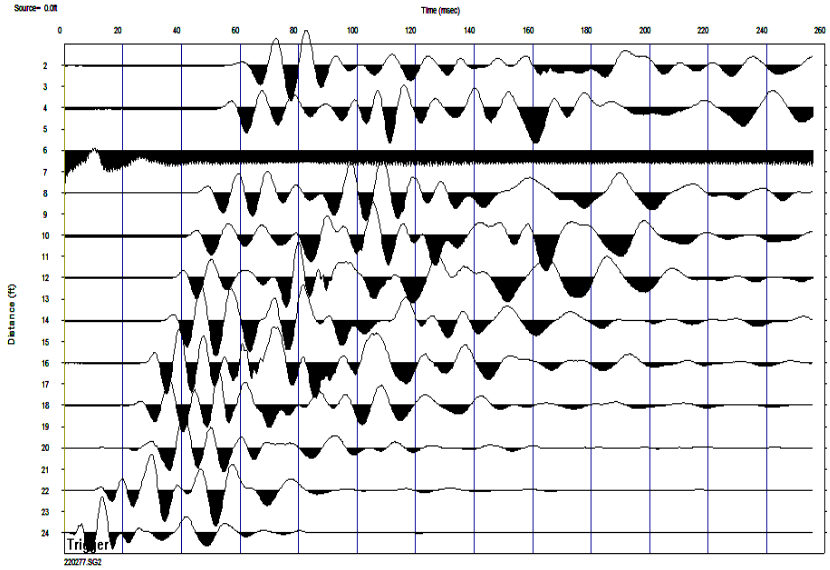

Fig. 7: Seismic wiggle showing reverse arrival time of P-wave curve for a 12-channel seismic line installed to the Seismic equipment from the study area

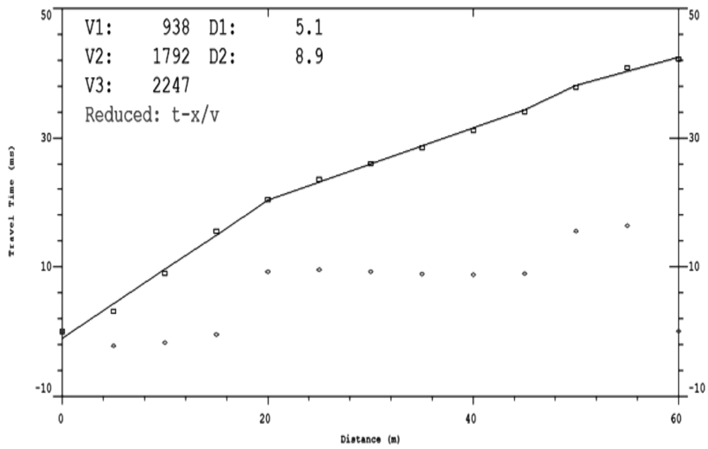

Fig. 8: T-X plot of Ababene 309 P F (RMS error <5%)

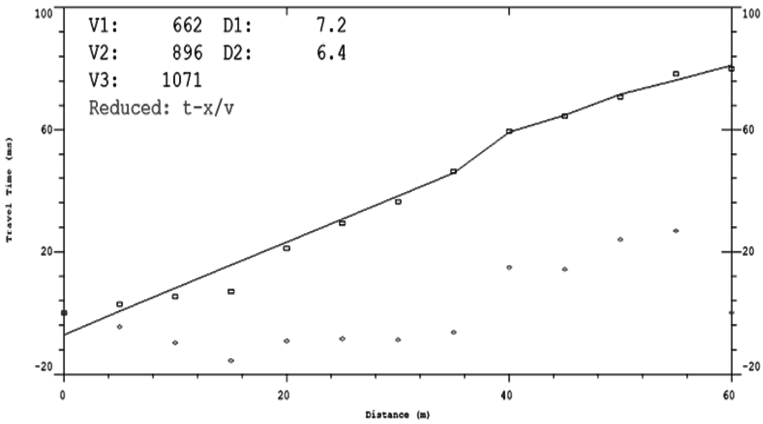

Fig. 9: T-X plot of Ababene 310 S F (RMS error <5%)

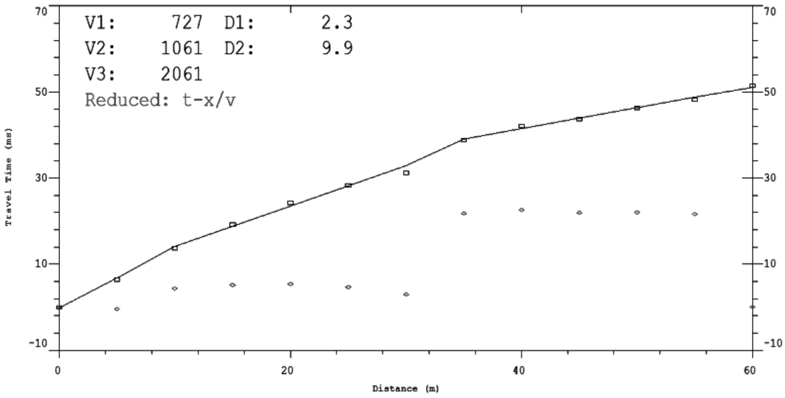

Fig. 10: T-X plot of Ababene 315 P R (RMS error <5%)

TABLE 2(a) Summary of results of seismic velocities and depth from Itigidi to Ekukunela

STUDY LOCATION	COORDINATES (°) LATITUDE	LONGITUDE	V_p (m/s)	V_{p2} (m/s)	V_{p3} (m/s)	V_s (m/s)	V_{s2} (m/s)	V_{s3} (m/s)	V_{p1}/V_{s1}	V_{p2}/V_{s2}	V_{p3}/V_{s3}	D_{p1} (m)	D_{p2} (m)	D_{s1} (m)	D_{s2} (m)
Itigidi	5.89833	8.02713	585	681	1017	385	441	509	1.52	1.54	2.00	3.8	8.8	6.2	1.7
Ediba	5.86469	8.03388	553	1695	2390	349	625	1246	1.58	2.71	1.92	3.8	7.5		
Ekurku	5.935	8.03513	584	1931	4831	411	1295	2122	1.42	1.49	2.28	3.1	12.2	6	6.8
Agbara	5.98611	8.01772	541	691		309	409		1.75	1.69		14.6		4.25	
Annong	5.887166	8.06061	728	1141	2806	482	655	1304	1.51	1.74	2.15	2.8	12.1	2.7	9
Usumutong	5.7663	8.01827	857	1069	1466	533	598	871	1.61	1.79	1.68	4.5	8.3	2.6	10.1
Pcn p/s Ijiman Ugep	5.80716	8.0846	690	1158	2251	475	527	675	1.45	2.20	3.33	4.2	10.9	2	5.3
st Theresas p/s Ugep	5.82236	8.08622	584	815	1931	313	480	705	1.87	1.70	2.74	4.9	10.7	2.5	9
Ekori	5.88002	8.12083	602	669		363	401		1.66	1.67		2		4.4	
Nkpani	5.8418	8.5663	658	946	1806	368	601	833	1.79	1.57	2.17	6.9	12.1	7.1	6.6
Onyadama	5.93388	8.23822	669	1471	2457	347	747	1247	1.93	1.97	1.97	7.3	8.7	4.8	8.6
Ababene	5.95102	8.26269	822	2524	2990	484	745	1272	1.70	3.39	2.35	25	2.3	5.1	9
Ovonum	5.98881	8.27063	634	1241	5368	454	615	799	1.40	2.02	6.72	4.6	8.6	4.2	5.9
Apiapum	5.99794	8.31577	960	1756	2572	444	460	649	2.16	3.82	3.96	5.5	5.2	2.5	7.7
Owakande	6.03394	8.34488	793	1448	2983	462	645	1100	1.72	2.24	2.71	8	9.9	4.8	8.6
st Francis p/s Obubra	6.8513	8.32841	621	697	1134	284	327	389	2.19	2.13	2.92	4.8	8.3	2.8	2.8
Iyamitet	5.85819	8.35508	763	1447	1574	408	740	714	1.87	1.96	2.20	4.1	0.5	2.7	0.5
Iyamoyong	5.97241	8.3588	732	808	1587	484	496	754	1.51	1.63	2.10	2.1	13.5	17.2	2.6
Ochon	5.92802	8.44227	1150	2275	4170	523	809	1155	2.20	2.81	3.61	6.4	7.6	3.1	11.4
onyen-okpon	5.97494	8.47261	782	1777	2908	282	399	715	2.77	4.45	4.07	4.2	7.3	5	6.5
Alesi	5.94891	8.51108	535	1049	2579	277	488	1111	1.93	2.15	2.32	4	7.9	4.4	9.4
Ekukunela	5.94458	8.53891	651	1347	3936	422	713	1064	1.54	1.89	3.70	5.1	9.9	3.5	4.2

TABLE 2(b) Summary of results of seismic velocities and depths from Omindom to Velos Ikom

STUDY LOCATION	COORDINATES (°) LATITUDE	LONGITUDE	V_P (m/s)	V_{P2} (m/s)	V_{P3} (m/s)	V_s (m/s)	V_{s2} (m/s)	V_{s3} (m/s)	V_{p1}/V_{s1}	V_{p2}/V_{s2}	V_{P3}/V_{S3}	d_{p1} (m)	d_{p2} (m)	d_{s1} (m)	d_{s2} (m)
Omindom	5.93555	8.58430	618	1816	4053	298	359	751	2.07	5.06	5.40	4.8	9.7	3.5	14.8
Ekpokpa	5.98825	8.61569	481	1468	3461	317	521	777	1.52	2.82	4.45	2.6	10	4.8	13.4
Akam	5.94422	8.62794	615	2109	4719	325	599	920	1.89	3.52	5.13	3.7	10.6	2.5	10.6
Abijang	5.82705	8.70941	643	1116	2719	443	547	778	1.45	2.04	3.49	2.7	3.7	1.1	6.4
Enoghi-ikom	5.95297	8.73680	297	499	2026	201	255	353	1.48	1.96	5.74	4.6	13.3	4.2	5.6
Grassfield	5.95250	8.73980	390	1174	3201	192	236	416	2.03	4.97	7.69	8.8	13	2.6	7.6
Kalime	5.90991	8.77533	715	1014	2622	342	353	674	2.09	2.87	3.89	4.2	12.1	1.9	14.0
Crin Ajasor	5.87644	8.81561	281	544	1640	192	323	395	1.46	1.68	4.15	4.6	7.5	8.5	12.1
Okondi-Ikom	5.96366	8.78847	1168	1737	2488	510	641	1214	2.29	2.71	2.05	2.4	5.4	6.8	8.0
Agbokim waterfall	5.90411	8.89425	610	1238	2169	286	310	421	2.13	3.99	5.15	8	8.8	2.3	7.8
Wula	6.39866	9.11140	360	378	1616	209	245	354	1.72	1.54	4.56	1.6	8.3	3	3.6
Bukalum	6.34269	9.11302	492	999	5968	325	451	671	1.51	2.22	8.89	4.2	16	5.6	7.5
Kanyang	6.26447	9.04694	387	960	2583	257	367	459	1.51	2.62	5.63	4.9	9.3	3.2	3.8
Abo Ogbante	6.16333	9.02102	433	770	2866	226	433	490	1.92	1.78	5.85	4.7	3.9	4.2	6.2
Bashua	6.08122	8.96272	619	908	2562	391	424	553	1.58	2.14	4.63	4.7	10	3.8	4.6
Biawan	6.07683	8.92170	494	1043	4020	314	430	637	1.57	2.43	6.31	9.8	14.9	5.9	7.0
Orim Ekpang	6.06597	8.89536	528	600	925	340	377	408	1.55	1.59	2.27	1.9	9.6	2.4	4.7
Bendege Ekim	6.01531	8.88000	459	1316	3058	260	350	627	1.77	3.76	4.88	5.5	8.7	5.3	8.2
Adijikpong	6.00800	8.74613	512	1225	3904	321	364	562	1.60	3.37	6.95	7.4	14.5	2.5	7.0
Akparabong	6.03147	8.74780	649	1567	2829	289	349	417	2.25	4.49	6.78	5.1	7.3	4.7	4.5
Velos Ikom	5.96516	8.71883	459	655	1139	255	336	472	1.80	1.95	2.41	5.9	9.9	4,7	10.6

TABLE 3 (a) Summary of results of elastic constants from Itigidi to Ekunela

STUDY LOCATION	COORDINATES (°) LATI TUDE	LONGI TUDE	DENSITY (kg/m^3) ρ_1	ρ_2	ρ_2	μ_1 $\times10^8$ (N/m^2)	μ_2 $\times10^8$ (N/m^2)	μ_3 $\times10^8$ (N/m^2)	E_1 $\times10^8$ (N/m^2)	E_2 $\times10^8$ (N/m^2)	E_3 $\times10^8$ (N/m^2)	K_1 $\times10^8$ (N/m^2)	K_2 $\times10^8$ (N/m^2)	K_3 $\times10^8$ (N/m^2)
Itigidi	5.89833	8.02713	2670	2670	2670	3.96	5.19	6.92	8.85	11.80	18.40	3.86	5.46	18.40
Ediba	5.86469	8.03388	2670	2670	2670	3.25	10.40	41.50	7.60	29.60	109.00	3.83	62.80	97.20
Ekureku	5.93500	8.03513	2670	2670	2670	4.51	44.80	120.00	9.10	97.70	332.00	3.09	39.90	463.00
Agbara	5.98611	8.01772	2670	2670		2.55	4.47		6.41	11.00		4.42	6.79	
Annong	5.88717	8.06061	2670	2670	2670	6.20	11.50	45.40	13.80	28.70	124.00	5.88	19.50	150.00
Usumutong	5.76630	8.01827	2670	2670	2670	7.59	9.55	20.30	18.00	24.30	49.70	9.50	17.80	30.40
Pcn p/s Ijiman Ugep	5.80716	8.0846	2670	2670	2670	6.02	7.42	12.20	12.60	20.30	35.30	4.68	25.90	119.00
St theresas p/s Ugep	5.82236	8.08622	2670	2670	2670	2.62	6.15	13.30	6.79	15.20	37.80	5.62	9.53	81.90
Ekori	5.88002	8.12083	2670	2670		3.52	4.29		8.54	10.50		4.99	0.06	
Nkpani	5.84180	8.5663	2670	2670	2670	3.62	9.64	18.50	9.20	22.40	50.60	6.74	11.00	62.40
Onyadama	5.93388	8.23822	2670	2670	2670	3.21		41.50	84.60	39.50	110.00	7.66	37.90	106.00
Ababene	5.95102	8.26269	2670	2670	2670	6.25	14.80	43.20	15.40	43.00	120.00	9.70	150.00	181.00
Ovonum	5.98881	8.27063	2670	2670	2670	5.50	10.10	17.00	10.70	27.00	50.70	3.39	27.70	747.00
Apiapum	5.99794	8.31577	2670	2670	2670	5.26	5.65	11.20	14.40	16.50	33.00	17.60	74.80	162.00
Owakande	6.03394	8.34488	2670	2670	2670	5.70	11.10	32.30	14.20	30.60	91.80	9.19	41.20	195.00
St Francis p/s obubra	6.8513	8.32841	2670	2670	2670	2.15	2.86	4.04	5.89	7.76	11.60	7.43	9.16	28.90
Iyamitet	5.85819	8.35508	2670	2670	2670	4.44	1.46	13.60	11.60	38.70	37.30	9.62	36.40	48.00
Iyamoyong	5.97241	8.3588	2670	2670	2670	6.25	6.57	15.20	13.90	15.70	41.10	5.97	8.67	47.00
Ochon	5.92802	8.44227	2670	2670	2670	7.30	17.50	35.60	20.00	49.90	100.00	25.60	115.00	417.00
Onyen-okpon	5.97494	8.47261	2670	2670	2670	2.12	4.25	13.60	6.05	12.50	40.10	13.50	78.60	208.00
Alesi	5.94891	8.51108	2670	2670	2670	2.05	6.36	33.00	5.40	33.00	91.40	4.91	20.90	134.00
Ekukunela	5.94458	8.53891	2670	2670	2670	4.75	13.60	30.20	10.80	35.40	88.30	4.98	30.30	373.00

TABLE 3 (b) Summary of results of elastic constants from Omindom to Velos Ikom

STUDY LOCATION	COORDINATES (°) LATI TUDE	LONGI TUDE	DENSITY (kg/m³) ρ_1	ρ_2	ρ_2	μ_1 ×10⁸ (N/m²)	μ_2 ×10⁸ (N/m²)	μ_3 ×10⁸ (N/m²)	E_1 ×10⁸ (N/m²)	E_2 ×10⁸ (N/m²)	E_3 ×10⁸ (N/m²)	K_1 ×10⁸ (N/m²)	K_2 ×10⁸ (N/m²)	K_3 ×10⁸ (N/m²)
Omindom	5.93555	8.58430	2670	2670	2670	2.37	3.44	15.10	6.39	10.20	44.60	7.04	8.35	419.00
Ekpokpa	5.98825	8.61569	2670	2670	2670	2.68	7.25	16.10	5.99	20.70	47.50	2.60	47.90	298.00
Akam	5.94422	8.62794	2670	2670	2670	2.82	9.58	22.60	7.37	27.90	66.90	6.34	106.00	564.00
Abijang	5.82705	8.70941	2670	2670	2670	5.24	7.99	16.20	11.00	21.40	47.00	4.05	22.60	176.00
Enoghi-ikom	5.95297	8.73680	2670	2670	2670	1.08	1.74	3.33	2.32	4.59	9.88	0.92	4.33	105.00
Grassfield	5.95250	8.73980	2670	2670	2670	0.98	1.49	4.62	2.64	4.40	13.80	2.75	34.80	267.00
Kalime	5.90991	8.77533	2670	2670	2670	3.12	3.33	12.10	8.44	9.52	35.50	9.49	23.00	167.00
Crin ajasor	5.87644	8.81561	2670	2670	2670	0.98	2.79	4.17	2.09	6.84	12.20	0.80	4.19	66.30
Okondi-ikom	5.96366	8.78847	2670	2670	2670	6.94	11.00	39.40	19.20	31.20	106.00	27.20	6.59	113.00
Agbokim waterfall	5.90411	8.89425	2670	2670	2670	2.18	2.57	4.73	5.94	7.53	14.00	7.02	3.75	119.00
Wula	6.39866	9.11140	2670	2670	2670	1.17	1.60	3.35	2.91	3.65	9.87	1.91	1.68	65.30
Bukalum	6.34269	9.11302	2670	2670	2670	2.82	5.43	1.20	6.28	14.90	35.90	2.70	19.40	935.00
Kanyang	6.26447	9.04694	2670	2670	2670	1.76	3.60	5.63	3.90	10.20	16.70	1.65	19.80	171.00
Abo Ogbante	6.16333	9.02102	2670	2670	2670	1.36	5.01	6.41	3.58	12.70	19.00	3.19	9.16	211.00
Bashua	6.08122	8.96272	2670	2670	2670	4.08	4.80	8.17	9.54	13.10	24.10	4.79	15.60	164.00
Biawan	6.07683	8.92170	2670	2670	2670	2.63	4.94	10.80	6.11	13.80	32.20	3.01	22.50	417.00
Orim ekpang	6.06597	8.89536	2670	2670	2670	3.09	3.79	4.44	7.07	8.91	12.30	3.33	4.55	16.90
Bendege ekim	6.01531	8.88000	2670	2670	2670	1.80	3.27	10.50	4.56	9.50	31.00	3.22	41.90	236.00
Adijikpong	6.00800	8.74613	2670	2670	2670	2.75	3.54	8.43	6.47	10.30	25.10	3.33	35.30	396.00
Akparabong	6.03147	8.74780	2670	2670	2670	2.23	3.25	4.64	6.14	9.59	13.80	8.27	61.20	207.00
Velos ikom	5.96516	8.71883	2670	2670	2670	1.74	3.01	5.95	4.43	7.97	16.60	3.31	7.44	26.70

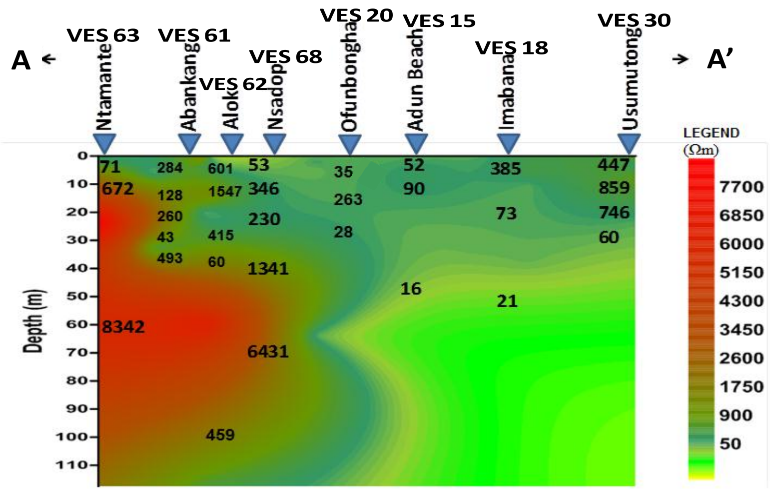

Fig. 11: Model showing AA’ Geoelectric Psuedosection of the study area

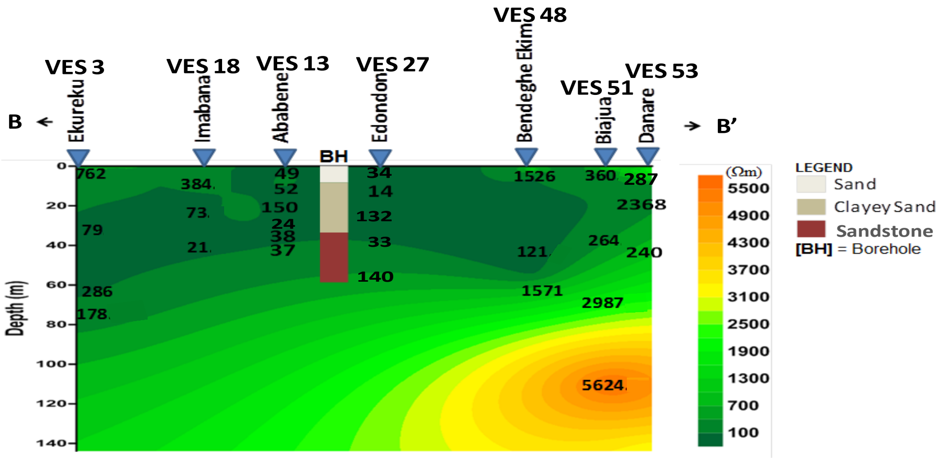

Fig. 12: Model showing BB' Geoelectric Pseudosection of the study area

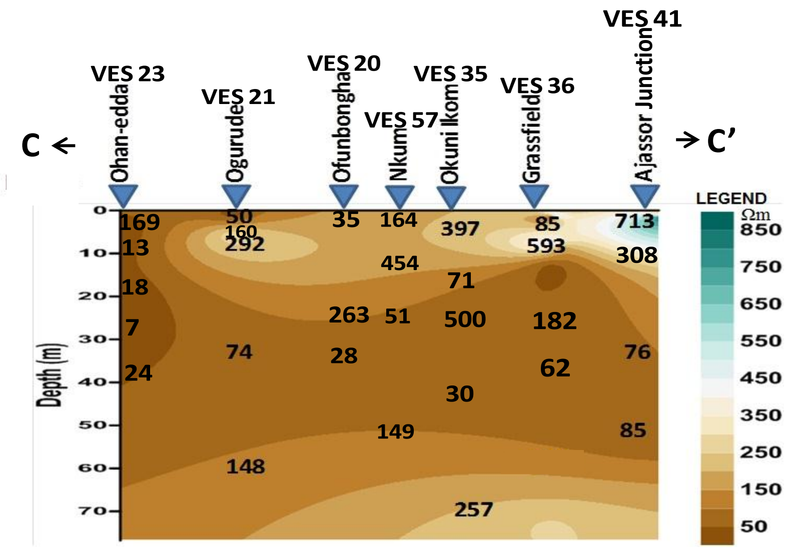

Fig. 13: Model showing CC' Geoelectric Pseudosection of the study area

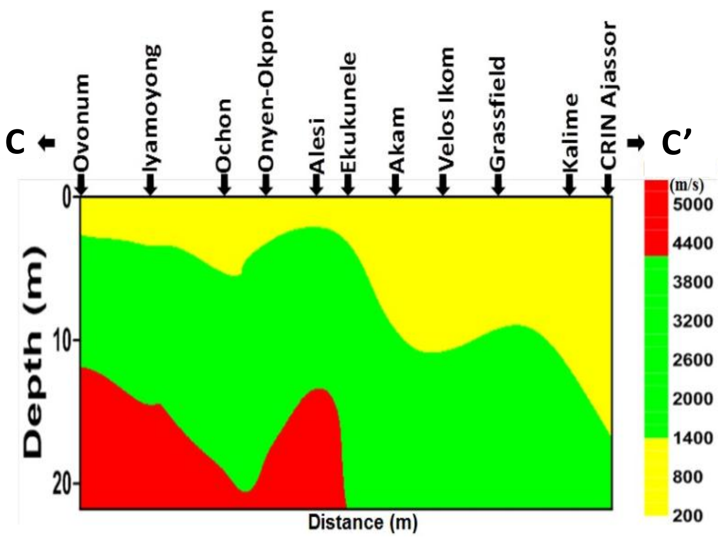

Fig. 14: Primary wave velocity variation with depth of CC' Geoseismic Pseudosection of the study area

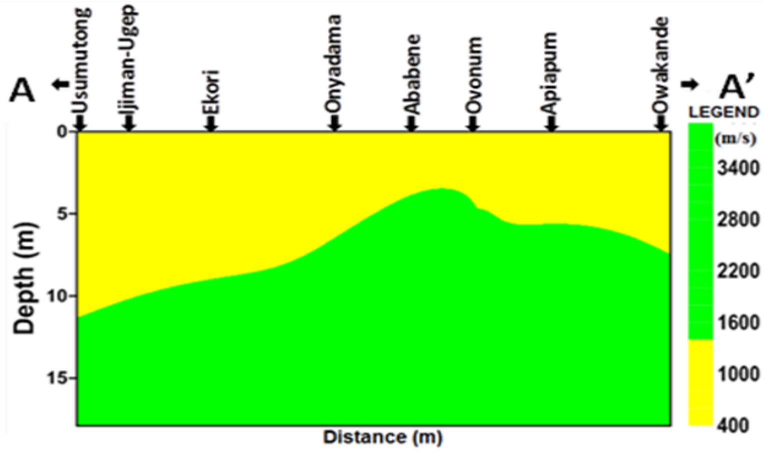

Fig. 15: P-wave velocity variation with depth: AA' Geoseismic Pseudosection of the study area

values around Alok and Nsadop presents a picture of a basement sedimentary contact, this contact is characterized by fractured basement and has the potential for water as indicated by the values of <10^4 Ωm which is the resistivity values for wet basement rocks (granite) (Loke and Dahlin, 1997).

Aquifers

Three geoelectrical sections were prepared for the study area (Figs. 11, 12 and 13), Fig. 11 is a geoelectrical section trending Northeast – Southwest marked AA' and shows the existence of thick aquifer units in the third layer with resistivity of 164 – 746 Ωm and thickness of 5.8 – 38m and lies within a depth of 30 – 70 m beneath the surface. Apart from the third layer, the fifth layer also constitutes one of the aquiferous units in some location. Fig. 12 is a geoelectric section trending East – West marked BB', it shows the third layer as the aquiferous unit with resistivity between 121 – 291 Ωm and thickness of 5.1 – 154.0 m, the resistivity range of these aquifer units suggests that the layer is dominated with sandy materials, the third layer in this geosection is highly variable and thins out greatly in some locations like Imabana (3.3 m) and Ababene (3.6 m), the thinning out of this lithostrata around Ababene and Imabana axis of the psuedosection results in a poor groundwater potential in this part of the profile.

The Northwest–Southeast geosection marked CC'is shown in Fig. 13, the third layer constitute the aquifer unit, with resistivity range of 74–257 Ωm and thickness of 4.8–39.8 m. The aquifer exists at a depth range of 27–75 m, which can easily be tapped by both private and cooperate developers.

Seismic Geosection

Two seismic refraction geosections were made as shown in Figs. 14 – 15. The first section (Fig. 14) which trends Northwest – Southeast marked CC' shows a conspicuous variation in primary wave velocity V_P with depth. Three distinct layers were imaged in the geosection. The first layer had a primary wave velocity of 281 m/s to 1,150 m/s and a thickness of 2.4 m to 4.6 m. within the layer a V_p range of 400 m/s to 600 m/s within a depth range of 1 m to 2 m is inferred as organic materials in the soil which could be loose sand/rubble/landfill/refuse/disturbed soil and clay landfill (http:pkukmwebukm.my/rohim). For road construction, this layer must be ripped off because it does not have sufficient bearing capacity (Okwueze, 1991).

The locations in the Southeast (SE) of the profile registered a first layer of up to 14m deep. There is a general increase in velocity (V_p) from the first layer to the second layer. This increase can be explained in terms of consolidation of the earth materials as one gets deeper. There is also a variation in primary wave velocity (V_p) within the second layer. The range of V_p is from 544 m/s to 2,275 m/s, with layer thickness ranging from 7.3 m to 13.6 m. The range of P-wave velocities of the layer when compared to borehole logs, suggest that at various locations, the layer is made up of laterite, sand, gravel, clay and shale. The third layer has a P-wave velocity range of 1,139 m/s to 5,368 m/s and thickness of 1.9 m to 17.2 m. It is inferred that sandy clay dominates the layer. There was no access to deeper refractors because of the limited energy of the source used in the survey.

The Northeast - Southwest profile marked AA' is shown in Fig. 15. Only two geoseismic layers were accessed. The first layer has a V_p range of 590 m/s to 960 m/s and a thickness range of 2.0 m to 8 m. This indicates that the top layer of this profile is chiefly dry loose sand (Alhasen et al., 2010). The bearing capacity of this layer to a depth of 3m is not sufficient enough for road construction and therefore should be ripped off. The second layer of the Southwest – Northeast section has a V_p range of 378 m/s – 2,524 m/s and a thickness range of 6.2 m to 13 m. It is adjudged to be more compacted and consolidated than the overlying layer because of the obvious velocity increase.

Generally the elastic constants varied very widely and anomalously. The shear modulus, μ, varied from 0.98 GPa to 120.00 GPa, while the bulk modulus varied from 0.06 GPa to 935.00 GPa. Also the Young's modulus varied from 2.09 GPa to 332.00 GPa. These variations defied the normal cause of hierarchy of values of elastic constants in many places, thus suggesting geologic environment with surfaces that are undulating, without clear-cut natural geologic boundaries, whose velocities might slowly vary both laterally and horizontally. These places with anomalous variations could account for the numerous failed roads in those areas. However, the V_p/V_s ratio for all the sites registered values that are greater than 1.5, which is generally indicative of porous or fractured rocks partially or fully saturated with fluid.

VI. Conclusion

Interpretation of the geoelectric sounding data showed characteristic curves with two to six geoelectric layers. The KH, HKH and HK curve types dominated the area with a prevailing frequencies of 23.7%, 16.96% and 11.86%. Evaluation of the reflection coefficient and resistivity contrast revealed that VES stations 6, 12, 26, 29, 36, 37, 45, 46, 47 and 60 might be areas with high density water fractures because their reflection coefficients and resistivity contrasts were not less than 0.9 and 19, respectively. There is a variation in the depth to water table in the study area. The trend of the variation is from Northeast to Southwest, with range of values of 10-50 m and 60-110 m, respectively.

Six geoelectric layers were obtained from the interpretation of the sounding data. The electrical resistivity of the first layer was between 100 Ωm and 2,115 Ωm which was indicative of clay/shale/sandy silt. The second layer resistivity was between 9.4 Ωm and 4,317.0 Ωm. This was inferred to be shalestone/shale. It was underlain by the third layer which had a resistivity range of 100-5422 Ωm, inferred as sandstone. The materials of this layer is indicative of an aquifer. The fourth layer had resistivity values that range from 10.6 Ωm to 6,415.0 Ωm. The fifth layer resistivity values were between 8.4 and 3,511.2 Ωm, while the last layer had resistivity values between 10.0 Ωm and 6,103.0 Ωm.

The productive shallow aquifer terrains in the study area according to borehole lithologic logs are made up of fine sands and sandstones with resistivity ranges of 100-500 Ωm and depth of 60 m. These shallow terrains are horizontally aligned in the study area. The deep aquifer terrains which consist of coarse grained sands and fractured basement, had resistivity range of 1000-2,500 Ωm and a depth from surface to bottom of about 150 m. The area has been identified to have confined aquifer terrain due to the confining clay layer which is of large vertical extent in the adjacent layers that enclosed the aquifer.

Analysis of the seismic refraction data revealed two to three geoseismic layers. The first layer had velocities values that are from 602 m/s to 960 m/s and depth values ranging from 1.5 to 8.0 m, which is indicative of sand (dry)/top soil/clay, when compared to nearby borehole data. The second layer had velocities of 378 m/s to 2,474 m/s and refractor depth that range from 1.3 m to 13.0 m. This layer is inferred to composed of clay/sand(water saturated, loose)/sand and gravel near surface based on nearby borehole logs. The third layer had velocity range of 1,587 m/s to 5,368 m/s, suspected to be weathered basement.

The elastic constants varied wildly and anomalously from site to site and from layer to layer, which is an indication of both lateral and vertical inhomogeneity. Some of the survey sites recorded high values of elastic constants especially bulk modulus and shear modulus . Rocks from such sites will not deform under elevated load. They provide foundation for durable roads. However, those sites with comparatively low elastic constants are vulnerable to road failures and as such should be excavated or treated before constructing civil engineering works. The S-wave velocity depends mainly on the properties of the rock matrix and is nearly independent of the pore fill whereas P-wave velocity depends on both matrix and pore fill Kirsch, 2009). Hence, the high values (> 1.5) of the ratio of V_p to V_s indicates that the soils and rocks have pores and fractures that are partially or fully filled with water.

References

[1]. Akpan, A. E. Ugbaja, A. N., George, N. J. (2013). Integrated Geophysical, Geochemical and hydrogeological investigation of shallow ground water resources in parts of the Ikom-Mamfe Embayment and the adjourning in Cross River State, Nigeria. Environ. Earth Sci. Doi:10/1007/s12665-013-2232-3.

[2]. Alhassan, D. U., Dangana, L. M. Salako, K. A. Jonah, S. A. & Ofor, N. P. (2010). Seismic Refraction investigation of the subsurface structure at the Southern part of Niger State, College of Education, Minna, Bayero Journal of Pure and Applied Sciences., **3(2)**, 56-61.

[3]. Ayolabi, E. A. (2004). Seismic refraction survey of University of Lagos, Nigeria and its implication. Journal of Applied Sciences, **7 (3)**, 4319-4327.

[4]. Ayolabi, E. A., Adeoti, L. Oshinlaja, N. A. Adeosun, I. O., & Idowu, O. I. (2008). Journal of Science Research and development 2008/2009, **11,** 42-61.

[5]. Benkhelil, M. G., Ponsard, J. F. Saugy, L. (1975). The Bornu-Benue Trough, The Niger Delta and its offshore Tectono-sedimentary reconstruction during the cretaceous and Tertiary from geophysical and geology. In: Kogbe CA (ed) Geology of Nigeria. Elizabethan Press, Lagos. pp.277-309.

[6]. Bernard, J. (2003). Short notes on depth of investigation of electrical methods. www.iris-instruments.com

[7]. Bhathacharya, P. K., Patra, H. P. (1986). Direct current geoelectric sounding: principles and interpretation. Elsevier Science Publishing Co. Inc., Amsterdam.
[8]. Burton, A. N. (1976). The use of geophysical methods in Engineering Geology, Part 1: Seismic Techniques. Ground Engineering.
[9]. Chakravarthi, V. Shankar, GBK., Muralikharan, D., Harinarayana, T., Sundarajan, N. (2007). An integrated geophysical approach to imaging subbasal Sedimentary Basin: case study of Jam River Basin, India: Geophysics, 72(6):B141-B147. doi:10.1190/12777004.
[10]. Cross River Basin Development Authority (CRBDA) (1982). Inventory of Natural Site conditions, soils slopes, hydrology, landuse and vegetation throughout the area of operation of the authority. Technical report 4.
[11]. Drake, C. L. (1962). Geophysics and Engineering, Geophysics **27**, 193-197.
[12]. Early, K. R. and Dyer, K. R. (1964). The use of resistivity survey in foundation site underlain by Karst dolomite, Geotechnique **14**, 341-348.
[13]. Edet, A. E., Nganje, T. N., Ukpong, A. J. Ekwere, A. S. (2011). Groundwater chemistry and quality of Nigeria: A Status Review. African Journal of Environmental Science and Technology. **5(13)**:1152-1169, DOi:10.5897/AJESTX11.011.
[14]. Eseme, E., Agyingi, C. M., Foba-Tendo, J. (2002). Geochemistry and genesis of brime emanation from cretaceous strata of the Mamfe Basin, Cameroun, J. Afri. Earth Sc. **35**, 467-4776 doi:10/1016/50899-55362(2)00171-9.
[15]. Geosoft W., (2001). Seismic Refraction processing software for Windows, Instruction manual, Geosoft Geological and geophysical Software. Geneva: Lully.
[16]. Http://pkukmwebukm.my/rohim
[17]. Keary, P. & Brooks, M. (1984). An introduction to geophysical exploration. Blackwell Scientific publication, Oxford, pp. 198-217.
[18]. Kirsch, R. (2009). Groundwater geophysics – a tool for hydrology. Springer – Verlag, Berlin, pp. 548.
[19]. Kurtenacker, K. S. (1934). Some practical application of resistivity measurement to highway problem. Transaction of American Institute of Mining and Metallurgical Engineers, **110**, 193-205.
[20]. Loke, M. H. & Dahlin, T. (1997). A combined Gauss-Newton and Quasi-Newton inversion method for the interpretation of apparent resistivity pseudosections. Procedures of 3rd meeting of the European Association of Environmental and Engineering Geophysics, 8-11 September, 1997, Aarhus, Denmark, 139-142.
[21]. Loke, M. H. (2001). RES ID version 1.0 for Windows 95/98/ME/2000/NT, I-D Resistivity. IP and SP inversion and forward modeling for Wenner and Shlumberger arrays.
[22]. Martinez, A. G., Takahashi, K. Nunez, E. Silva, Y, Trasmonte, G. Mosquera, K. Lagos, P. (2008). A multi-institutional and interdisciplinary approach to the assessment of vulnerability and adaptation to climate change in the Peruvian Central Andes: Problems and prospects. Adv. Geosci. J. **14**, 257-260.
[23]. Nigeria Geological Survey Agency (NGSA) (2006). Geological and mineral resources map of Cross River State, Nigeria.
[24]. Nunn, K. R. (1979). Geophysical survey at two landfill sites in the west midlands. Symposium on the engineering behaviour of industrial and urban hill.
[25]. Odigi, M. I., Amajor, L. C. (2009). Geochemical characterization of cretaceous sandstones from the southern Benue Trough, Nigeria. Chin. J. GEochem. **28**, 044-054. Doi:10.1007/s11631-009-00447.
[26]. Odoh, B. I. (2010). Surface-outcrop characterization for fracture flow of groundwater: case study of ABakaliki Basin, Ebonyi State, Nigeria. Int. Arch. Appl. Sci. Technol. **1(1)**:45-53.
[27]. Offodile, M. E. (1975). A review of the geology and cretaceous of the Benue valley. In Kogbe CA (ed) Geology of Nigeria; Elizabethan Press Lagos, pp.375-376.
[28]. Okwueze E. E. (1991). Shear wave observation in seismic refraction prospecting. Journal of mining and Geology, 24(1&2).
[29]. Olorunfemi, M. O. and Meshida, E. A. (1987). Engineering Geophysics and its application in Engineering site investigations (Case study from Ile-Ife area). The Nigerian Engineer. **22**, 57-66.
[30]. Orellana, E., and Mooney, H. (1966). Master tables and curves for vertical electrical soundings over layered structures of Madrid, Interciencia: India.
[31]. Petters, S. W. (1989). A regional hydrogeological study of rural water supply options for planning and implementation of phase II rural water programme in Cross River State. Unpublished Technical report submitted to DIFFRI, Cross River State.
[32]. Petters, S. W., Okereke, C. S., Nwajide, C. S. (1987). Geology of the Mamfe Rift, south eastern Nigeria. In Mathesis, G. Shandemerer J. (eds) Current research in African Earth Sciences, Balkema Rotterda. pp. 299-302.
[33]. Rapti-Caputo, D. (2010). Influence of climate change and human activities on the salinization process of coaster aquifer systems. Italan J. Agron. **5(3)**, 67-79.
[34]. Riddel, E. S. Lorentz, S. A., Kotze, D. C. (2010). A geophysical analysis of hydro-geomorphic controls within a headwater wetland in a granitic landscape, through ERI and IP. J. HYdrol Earth Sci.14:1697-1713. doi:10.5194/hess-14-1697-2010.
[35]. Roy, A. & Apparao, A. (1971). Depth of investigation in direct current methods. Geophysics, **36(5)**, 943-959.
[36]. Telford, W. W., Geldart, L. P. Sheriff, R. E., and Keys, D. A. (1990). Applied Geophysics. New York: Cambridge University Press.
[37]. Vender Velpa, BPA. (1988). A computer processing package for DC Resistivity interpretation for IBM compatibles, ITC Journal 4, The Netherlands.
[38]. Wagner, G., Zechauser, R. J. (2011). Climate policy: hard problem, soft thinking, Climate Change. doi:10.1007/s1054-011-0067-z.
[39]. Zohdy, A. A. R., Eaton, G.P & Mabey, D. R. (1980). Application of surface geophysics to groundwater investigations. U.S. Government printing office: Washington D.C.